Zhao, X., Liu, W., Liu, S., Zou, Y., and Chen, Q. 2017. "Inverse design of an indoor environment by using a CFD-based adjoint method with adaptive step size for adjusting design parameter" *Numerical Heat Transfer, Part A: Applications*, 71(7): 707-720.

Inverse Design of an Indoor Environment by Using a CFD-based Adjoint Method with Adaptive Step Size for Adjusting Design Parameters

Xingwang Zhao[a], Wei Liu[a,b], Sumei Liu[a], Ying Zou[a], and Qingyan Chen[b,a*]
[a]*Tianjin Key Laboratory of Indoor Air Environmental Quality Control, School of Environmental Science and Engineering, Tianjin University, Tianjin 300072, China*
[b]*School of Mechanical Engineering, Purdue University, West Lafayette, IN 47907, USA*
*Corresponding email: yanchen@purdue.edu
Address: 585 Purdue Mall, West Lafayette, IN 47907-2088, U.S.A.
Phone: +1 (765) 496-7562
FAX: +1 (765) 494-0539

Abbreviated title: Inverse design indoor environment with adaptive step size

Abstract

The step size used in the CFD-based adjoint method has a significant effect on the computing time. The constant step size usually used is obtained through a time-consuming trial-and-error process. This study used an adaptive step size for adjusting the design parameters in the CFD-based adjoint method. In order to validate the performance of the CFD-based adjoint method with the adaptive step size, this investigation evaluated three different inverse design cases with mixed convection flow. Our results confirmed that the adaptive step size is computationally efficient and can be used for inverse design of an indoor environment.

Keywords: Inverse design; Adjoint method; Computational fluid dynamics; Adaptive step size

Nomenclature

A	source item in the adjoint momentum equations
B	source item in the adjoint energy equation
D (**V**)	the rate of strain tensor
g	the gravity vector
J	objective function
J_{k-1}, J_k, J_{k+1}	objective function at previous, current and succeeding design cycle, respectively
K	Lipschitz constant
L	augmented objective function
N	incompressible Navier-Stokes equations in vector form
N_1	continuity equation
N_2, N_3, N_4	momentum equations
N_5	energy equation
p	air pressure
P_a	adjoint pressure
T	air temperature
T_0	desired air temperature on a design domain
T_a	adjoint temperature
T_{fl}	floor temperature
T_{inlet}	inlet air temperature
T_{max}, T_{min}	the maximum and minimum temperatures of the experimental

boundary condition, respectively

T_{op}	operating air temperature
T_r	roof temperature
T_w	wall temperature
$\mathbf{V}$	air velocity
$\mathbf{V}_0$	desired air velocity on a design domain
$\mathbf{V_a}$	adjoint velocity
$\mathbf{V}_{inlet}$	inlet air velocity
$V_{x,\,inlet}$, $V_{y,\,inlet}$, $V_{z,\,inlet}$	inlet air velocity in x, y and z directions, respectively
α, β	weighting factors
γ	air thermal expansion coefficient
δ	small constant set by the designer
Θ	design domain
κ	effective thermal conductivity
λ	the step size
λ_k	the step size in the k^{th} design cycle
Λ	the local Lipschitz constant
Λ_k	the local Lipschitz constant in the k^{th} design cycle
ν	effective viscosity
ξ	design parameters
ξ_{k-1}, ξ_k, ξ_{k+1}	design parameters at previous, current and succeeding design cycle, respectively

1. Introduction

Since people spend roughly 87% of their daily lives indoors [1], it is essential to design heating, ventilation, and air-conditioning (HVAC) systems to provide healthy and comfortable environments inside buildings [2]. The traditional method of designing HVAC systems uses a trial-and-error process. The designer first assumes air supply parameters according to his or her experience. A suitable method such as computational fluid dynamics (CFD) is then used to determine whether the resulting indoor environment would meet the thermal comfort and indoor air quality requirements. If not, the designer must adjust the air supply parameters iteratively until the indoor environment is satisfactory. In order to design a desirable indoor environment more effectively, one can use an inverse design method that seeks optimal air supply parameters for the HVAC system according to the design objective [3].

An inverse design method can combine CFD with an optimization algorithm. CFD is a commonly used and accurate means of determining the air distribution [4]. The optimization algorithm can be a genetic algorithm (GA) [5] or adjoint method [6]. The GA method is capable of finding the global optimal solution, but its computing time is proportional to the number of design parameters. As the number of design parameters increases, the computing cost can be very high. The adjoint method is more efficient than the GA method because it computes the gradient of the objective function with respect to the design parameters. The computing time for the adjoint method does not change with the number of design parameters [3]. The computing cost for this method is lower than that for the GA method, but it is still considerable. To further decrease the computing cost, a reduced-order method, such as the proper orthogonal decomposition method (POD) [7], can be used to replace CFD. However, reduced-order methods are not as accurate as CFD. Chen et al. [8] compared different inverse design methods and found the CFD-based adjoint method to be superior in terms of accuracy

and computing cost. Therefore, we selected this method for further study.

The CFD-based adjoint method calculates the gradient of the design objective function with respect to the design parameters. The gradient provides the direction in which to adjust the design parameters so that the design objective can be satisfied. This process also requires the determination of an appropriate step size for adjusting the design parameters, which is an important factor in the computing cost. A constant step size [9] for optimizing the design parameters has been widely used in many optimization designs, such as duct shape [10], turbine blades [11], hydraulic turbomachines [12], hydrofoils [13], and indoor environments [14]. These studies used a relatively small step size because an overly large step size would decrease the accuracy and numerical stability. However, a too-small step size requires more design cycles to obtain the optimal design. A constant step size is determined by experience or by a time-consuming trial-and-error process.

An alternative is to use an adaptive step size [15] to automatically adjust the design parameters in each design cycle [16]. For example, a number of previous studies have used an adaptive step size to design an optimal airfoil [17, 18, 19]. The results show that a design with an adaptive step size can provide the appropriate step size automatically in the inverse design process. However, an adaptive step size has not yet been used for adjusting design parameters for indoor environments. This paper explains how an adaptive step size can be determined and demonstrates its use in the design of different indoor environments.

2. Research Method

This section explains the CFD-based adjoint method and the use of an adaptive step size to adjust design parameters.

2.1 CFD-based adjoint method

To inversely design a desired indoor environment by the CFD-based adjoint method, this study first needs to establish a design objective function. For example, if the design objective is to produce a desired air velocity $\mathbf{V}_0$ (vector) and air temperature T_0 on a design domain, Θ, the corresponding objective function could be:

$$J(\xi) = \alpha \int_{\Theta} \left|\mathbf{V} - \mathbf{V}_0\right|^2 d\Theta + \beta \int_{\Theta} \left(T - T_0\right)^2 d\Theta \tag{1}$$

where $\mathbf{V}$ and T are the calculated air velocity and temperature, respectively, in the design domain; α and β the weight factors used to determine the relative importance of the two integrals in the equation; and $\xi = (\mathbf{V}_{inlet}, T_{inlet})$ a vector that denotes the design parameters, such as the air velocity and temperature from the inlet of the indoor space. The goal of the design is to minimize the objective function.

The adjoint method starts with an initialized design variable ξ, so that the $\mathbf{V}$ and T on the design domain can be obtained by solving the Navier-Stokes equations with CFD:

$$N_1 = -\nabla \cdot \mathbf{V} = 0 \tag{2}$$

$$(N_2, N_3, N_4)^T = (\mathbf{V} \cdot \nabla)\mathbf{V} + \nabla p - \nabla \cdot (2\nu D(\mathbf{V})) - \gamma \mathbf{g}(T - T_{op}) = 0 \tag{3}$$

$$N_5 = \nabla \cdot (\mathbf{V}T) - \nabla \cdot (\kappa \nabla T) = 0 \tag{4}$$

where $\mathbf{N} = (N_1, N_2, N_3, N_4, N_5)^T$ represents the incompressible Navier-Stokes equations in

vector form, p the air pressure, ν the effective viscosity, $D(\mathbf{V}) = (\nabla\mathbf{V}+(\nabla\mathbf{V})^T)/2$ the rate of strain tensor, κ the effective thermal conductivity, $\mathbf{g} = (0, 0, 9.81)$ m/s^2 the gravity vector, γ the thermal expansion coefficient of air, T the air temperature, and T_{op} the operating air temperature. Next, the objective function is calculated to determine whether it is sufficiently small. If not, we need to calculate the gradient of the objective function over the design parameters in order to adjust the parameters to minimize the objective function. Since the design parameters are not explicitly included in the objective function, we cannot find the relationship between the objective function and the design parameters directly. To solve for the gradient, the adjoint method introduces an augmented objective function L:

$$L = J + \int_\Omega \left(P_a, \mathbf{V_a}, T_a\right)\mathbf{N}d\Omega \tag{5}$$

where P_a, $\mathbf{V_a}$, and T_a represent the adjoint pressure, adjoint velocity, and adjoint temperature, respectively. Because $\mathbf{N} = 0$, the adjoint method calculates $dL/d\xi$ instead of $dJ/d\xi$. The gradient of the augmented objective function over the design parameters can be expressed as:

$$\frac{dL}{d\xi} = \frac{\partial L}{\partial \xi} + \frac{\partial L}{\partial \mathbf{V}}\frac{\partial \mathbf{V}}{\partial \xi} + \frac{\partial L}{\partial P}\frac{\partial P}{\partial \xi} + \frac{\partial L}{\partial T}\frac{\partial T}{\partial \xi} \tag{6}$$

Because the direct calculation of the gradient of the augmented objective function over the air velocity $\mathbf{V}$, air temperature T, and pressure P is very difficult, the adjoint method sets the last three terms of Eq. (6) to zero:

$$\frac{\partial L}{\partial \mathbf{V}}\frac{\partial \mathbf{V}}{\partial \xi} + \frac{\partial L}{\partial P}\frac{\partial P}{\partial \xi} + \frac{\partial L}{\partial T}\frac{\partial T}{\partial \xi} = 0 \tag{7}$$

Eq. (7) can be used to derive the adjoint equations. The detailed derivation procedure can be found in [14]. Here we only provide the final form of the adjoint equations:

$$-\nabla\cdot\mathbf{V_a} = 0 \tag{8}$$

$$-\nabla\mathbf{V_a}\cdot\mathbf{V} - \left(\mathbf{V}\cdot\nabla\right)\mathbf{V_a} + \nabla P_a - \nabla\cdot\left(2\nu D\left(\mathbf{V_a}\right)\right) - T\nabla T_a + \mathbf{A} = 0 \tag{9}$$

$$-\left(\mathbf{V}\cdot\nabla\right)T_a + \nabla\cdot\left(\kappa\nabla T_a\right) - \gamma\left(\mathbf{V_a}\cdot\mathbf{g}\right) + B = 0 \tag{10}$$

$$\mathbf{A} = \begin{cases} 2\alpha\left(\mathbf{V}-\mathbf{V}_0\right) & \text{for design domain } \Theta \\ 0 & \text{for domain } \Omega\setminus\Theta \end{cases} \tag{11}$$

$$B = \begin{cases} 2\beta\left(T-T_0\right) & \text{for design domain } \Theta \\ 0 & \text{for domain } \Omega\setminus\Theta \end{cases} \tag{12}$$

After solving the Navier-Stokes equations and the adjoint equations, we can calculate the gradient of the augmented objective function over the design parameters by:

$$\frac{dL}{d\xi} = \frac{\partial J}{\partial \xi} + \int_\Omega \left(P_a, \mathbf{V_a}, T_a\right)\frac{\partial \mathbf{N}}{\partial \xi}d\Omega \tag{13}$$

Finally, we use the steepest descent method [20] to adjust the design parameters:

$$\xi_{k+1} = \xi_k - \lambda_k \frac{dL}{d\xi_k} \tag{14}$$

where λ is the step size. With the new design parameters, the method solves the Navier-Stokes equations again to obtain new **V** and T on the design domain. If the objective function is sufficiently small, the inverse design process stops. Otherwise, the gradient of the augmented objective function over the design parameters is calculated again to adjust the design parameters. This process is repeated until the objective function becomes sufficiently small. Figure 1 shows the flow chart of the CFD-based adjoint method.

Note that the step size λ in Eq. (14) is constrained by a Lipschitz constant K ($K \geqslant 0$) [9]. The Lipschitz constant is a constant that satisfies:

$$K \geq \max \frac{\left| \frac{dL(\xi_k)}{d\xi_k} - \frac{dL(\xi_{k-1})}{d\xi_{k-1}} \right|}{\left| \xi_k - \xi_{k-1} \right|}, \qquad k = 2,3,4,... \tag{15}$$

Then the step size is determined by

$$\lambda = \frac{1}{2K} \tag{16}$$

For a given practical problem, the Lipschitz constant is not known before the design has been completed. This is probably the reason for previous investigators' use of a constant step size with the trial-and-error method; they sought to avoid oscillations and obtain steepest descent convergence. Since the trial-and-error method is time consuming, an adaptive step size should be used to determine the appropriate λ in each design cycle.

2.2 Adaptive step size

An adaptive step size for adjusting design parameters can be determined by exact line search or inexact line search [21, 22]. An exact line search determines the optimal step size by setting the gradient of the objective function over the step size to zero [23]. This is done because the objective function is dependent only on the step size λ once the design parameters have been initialized. However, in the design of an indoor environment, the gradient of the objective function over the step size cannot be obtained. Therefore, this study has used an inexact line search to determine the appropriate step size.

The inexact line search provides a non-optimal step size [24] that produces a reasonable decrease in the objective function. This type of search can be divided into two categories. One category involves finding a step size that satisfies the implicit restrictive inequality constraints. These constraints contain the Goldstein rule [15], the Wolfe rule [25], and the Armijo rule [9]. In each design cycle, an initial step size λ_k is used to calculate the objective function J_{k+1} and the gradient $dJ_{k+1}/d\xi_{k+1}$ of the succeeding step. If λ_k, J_{k+1}, and $dJ_{k+1}/d\xi_{k+1}$ do not satisfy the restrictive inequality constraints, one must adjust the step size λ_k until the restrictive inequality constraint is satisfied. It is again a trial-and-error process that requires many calculations and the storage of a large amount of data in each design cycle. The other search category uses the local Lipschitz constant to determine the step size adaptively. This category includes the GDAM method and the GDAM-2 method [16]. Since the GDAM-2

method contains the Wolfe rule and would again require significant computational effort, this study used the GDAM method to determine the step size adaptively. The GDAM method is a simple and explicit method that has less restrictive assumptions than the other methods, and therefore it is suitable for practical problems.

The GDAM method calculates the local Lipschitz constant in each design cycle by

$$\Lambda_k = \frac{\left\| \frac{dL(\xi_k)}{d\xi_k} - \frac{dL(\xi_{k-1})}{d\xi_{k-1}} \right\|}{\left\| \xi_k - \xi_{k-1} \right\|} \tag{17}$$

The calculation requires only the gradient of the objective function over the design parameters, and the design parameters at the current and previous steps. Then the step size in the k^{th} design cycle is determined by

$$\lambda_k = \frac{1}{2\Lambda_k} \tag{18}$$

The adaptive step size for adjusting design parameters is implemented in the CFD-based adjoint method. The CFD simulation uses the RNG k-ε model to simulate the turbulence flow in the indoor environment [26]. The convection terms in the Navier-Stokes equation and the adjoint equations are discretized by the first-order upwind scheme, and the diffusion terms are discretized by the central difference scheme. The Navier-Stokes equations and the adjoint equations are implemented and solved by the Open Source Field Operation and Manipulation (OpenFOAM) [27]. This study adopted the Boussinesq approximation [28] to simulate the buoyancy effect. The convergence criterion was set as $|J_k - J_{k-1}| < \delta$, where k is greater than or equal to 2 and δ is a small constant set by the designer.

3. Results

In order to validate the performance of the CFD-based adjoint method with the adaptive step size for adjusting design parameters, this study conducted an inverse design of the indoor environment for three cases. The first case was a two-dimensional (2D) ventilated cavity [29], the second case was a three-dimensional (3D) room [30], and the third case was a three-dimensional (3D) office [31]. Considering the flow features in actual indoor environment, all three cases were with mixed convection. The last case was also with temperature stratification. These cases were selected to represent different complexity levels of indoor airflow. The CFD-based adjoint method with a constant step size was applied to design the three cases. This study first used the air supply velocity and temperature measured in the experiment to conduct forward CFD simulations. This study then defined the design domain in each of the cases and used the air velocity and temperature profiles/field calculated by CFD in a specific location of the flow domain as the design objective. Finally, the CFD-based adjoint method with the adaptive/constant step size for adjusting design parameters was used to inversely identify the air supply velocity and temperature. If these inversely identified parameters were the same as the ones used in the experimental cases, then the CFD-based adjoint method was validated.

3.1 Two-dimensional ventilated cavity

The first case was a 2D ventilated cavity [29] with a flow domain of 1.04 m × 1.04 m as shown in Figure 2. Air was supplied through an inlet in the left wall near the roof and exhausted through an outlet in the right wall near the floor. The inlet height was 0.018 m, and the outlet height was 0.024 m. The supply air velocity was $V_{x,\,inlet} = 0.57$ m/s and $V_{y,\,inlet} = 0$, and the supply air temperature $T_{inlet} = 15$ ºC. The roof and wall temperatures were $T_r = T_w = 15$ °C, and the floor temperature $T_{fl} = 35$ ºC. Because of the high floor temperature and low air supply temperature, the flow type in this case was mixed convection. The design parameters were the air velocity and temperature at the air supply inlet.

This study first conducted a forward CFD simulation using the above boundary conditions and then used the calculated air velocity and temperature in the design domain (the vertical line in the middle of the floor in Figure 2) as the design objective. This study did not use the experimental data along the design domain as the design objective because the CFD simulation was not very accurate, and thus the calculated air velocity and temperature in the design domain did not agree absolutely with the measured data. The small error in the CFD simulation could lead to some differences in the air supply velocity and temperature obtained in the inverse design.

In the inverse design by the CFD-based adjoint method with the adaptive/constant step size for adjusting the design variable, Eq. (1) was used as the objective function. The weighting factors α and β were defined by

$$\alpha = \frac{1}{V_{x,inlet}^2} \tag{19}$$

$$\beta = \frac{1}{\left(T_{max} - T_{min}\right)^2} \tag{20}$$

where $V_{x,\,inlet} = 0.57$ m/s, $T_{min} = 15$ ºC, and $T_{max} = 35.5$ ºC. The inverse design initialized the air supply velocity and temperature as $V_{x,\,inlet} = 0.8$ m/s, $V_{y,\,inlet} = 0$, and $T_{inlet} = 21.85$ ºC. The constant step sizes for adjusting the air supply velocity and temperature were 10 and 3, respectively, and were determined by trial and error, but the adaptive step size was calculated by Eq. (17).

Table 1 summarizes the air supply velocity and temperature and the corresponding values of the objective function obtained through the inverse design process. The optimal air supply parameters produced by the two inverse design methods are very close to each other and also to the experimental data. The objective function also tends toward zero, which is an indicator that the results were close to optimal. In addition, the two methods required almost the same number of design cycles. All of these findings indicate that the CFD-based adjoint method with an adaptive step size for adjusting design parameters can provide the same results as those obtained with a constant step size. It is important to note that the adaptive step size was determined automatically in this case, while the constant step size was based on our experience. In most cases, the constant step size would require a trial-and-error process, which can be time consuming.

3.2 Three-dimensional ventilated room

The second case used to validate the performance of the CFD-based adjoint method with an adaptive step size for adjusting design parameters was a 3D ventilated room with dimensions of 2.44 m × 2.44 m × 2.44 m [30], as shown in Figure 3. Air was supplied through an inlet in the left wall near the ceiling and exhausted through an outlet in the right

wall near the floor. The inlet and outlet heights were 0.03 m and 0.08 m, respectively. The air supply velocity was $V_{x,\,inlet}$ = 1.366 m/s, $V_{y,\,inlet}$ = 0, and $V_{z,\,inlet}$ = 0, and the air supply temperature T_{inlet} = 22.2 ºC in the experiment. There was also a box with dimensions of 1.22 m × 1.22 m × 1.22 m at the center of the floor that was heated at 700 W to represent indoor heat sources. Other boundary conditions, such as surface temperatures, can be found in [30].

The objective function for the 3D ventilated room was again Eq. (1). The desired air velocity $\mathbf{V}_0$ (vector) and air temperature T_0 on the design domain Θ (the vertical line in the center of the room above the box as shown in Figure 3) were obtained by a forward CFD simulation using the boundary conditions in the experiment. The weighting factors on the objective function, α and β, were defined by Eqs. (19) and (20), respectively, where $V_{x,\,inlet}$ was 1.366 m/s, T_{min} was 22.2 ºC, and T_{max} was 36.7 ºC. The air supply velocity and temperature were used as design parameters. The initial conditions used in the inverse design process were randomly assumed to be $V_{x,\,inlet}$ = 2 m/s, $V_{y,\,inlet}$ = 0, $V_{z,\,inlet}$ = 0, and T_{inlet} = 27 ºC. The constant step sizes for adjusting the air supply velocity and temperature were 100 and 50, respectively, after several trial-and-error iterations, while the adaptive step size was calculated by Eq. (17).

Figure 4 illustrates the change in the objective function with the design cycle. The constant step size for adjusting the design parameters converged at the 15th design cycle, which satisfied the convergence criterion of $|J_k - J_{k-1}| < 0.01$, and the adaptive step size converged at the 25th design cycle. In this case, the convergence speed with the constant step size was faster, and the convergence was more stable, than with the adaptive step size. However, the speed and stability came with a price. Since the constant step size method required a large amount of time to obtain the step size, it was actually more time consuming. By contrast, the adaptive method determined the step size automatically in each design cycle, which was very effective. However, the step size that was obtained may not have been ideal. For example, as shown in Figure 5(a), the gradient of the objective function over the air supply temperature with the adaptive step size fluctuated more significantly than that with the constant step size. This in turn led to a large fluctuation of the air supply temperature as depicted in Figure 6(a). Nevertheless, as illustrated in Figure 5(b), the gradient of the objective function over the air supply velocity in the x direction approached zero quickly. The change in the air supply velocity in the x directionalso converged rapidly, as shown in Figure 6(b).

Table 2 shows that the inverse designs with the two methods converged to the same solution. The corresponding objective function was close to zero. The calculated air supply conditions were very close to the experimental data. The adaptive/constant step size methods were able to identify the optimal air supply parameters with similar accuracy. As discussed above, the CFD-based adjoint method with the adaptive step size for adjusting design parameters was much more computationally efficient than that with the constant step size.

We also performed a forward CFD simulation with the air supply parameters in Table 2. Figure 7 compares the simulated and calculated air velocity and temperature profiles in the design domain. For each parameter, the three profiles were quite similar because the optimal air supply parameters that were identified did not differ greatly from the experimental data. Figure 8 illustrates the corresponding air velocity distribution at the mid-z cross-section (the plane shown in Figure 3). The length of the arrows in the figure indicates the magnitude of the air velocity. The three air velocity distributions were almost identical. This result further confirms that the CFD-based adjoint method can be used to inversely identify the design parameters.

3.3 Three-dimensional ventilated office

The last case used for validating the CFD-based adjoint method was a 3D office with displacement ventilation [31] that was close to an actual office, as shown in Figure 9. The flow domain had dimensions of 5.16 m × 3.65 m × 2.43 m. The air was supplied at a low speed through an inlet in the middle of the right wall near the floor; it then traveled upward because of thermal buoyancy; and finally it was exhausted through an outlet in the center of the ceiling. The sizes of the inlet and outlet were 1.1 m × 0.53 m and 0.43 m × 0.43 m, respectively. The office also contained two occupants, two tables, two personal computers, two file cabinets, and six fluorescent lamps. The air supply velocity was $V_{x,\,inlet} = 0.09$ m/s, $V_{y,\,inlet} = 0$, and $V_{z,\,inlet} = 0$, and the air supply temperature $T_{inlet} = 17$ ºC. All other thermal boundary conditions and geometric dimensions can be found in [31].

In a similar manner to that in the previous two cases, we conducted a forward CFD simulation to obtain the air velocity and temperature in the design domains (the three thick vertical lines in Figure 9) as the design objective. The objective function was again Eq. (1), and the weighting factors α and β were defined by Eqs. (19) and (20), respectively, with $V_{x,\,inlet} = 0.09$ m/s, $T_{min} = 17$ ºC, and $T_{max} = 26.7$ ºC. The inverse design started randomly with initial conditions of $V_{x,\,inlet} = 0.15$ m/s, $V_{y,\,inlet} = 0$, $V_{z,\,inlet} = 0$, and $T_{inlet} = 22$ ºC from the inlet. After a few trial-and-error tests, the constant step sizes for adjusting the air supply velocity and temperature were set at 50 and 2, respectively, while the adaptive step size was calculated by Eq. (17). The design parameters were the air velocity and temperature at the air supply inlet.

Figure 10 shows the change in the objective function with the design cycle. The convergence for this case was quite elegant. As in the case of the 3D room, the inverse design with the constant step size for adjusting the design parameters was more stable than that with the adaptive step size; the results are shown in Figure 11. Again, this stability was achieved by several trial-and-error runs with the constant step size.

Even for such a complex case, the results in Table 3 show that the inverse design method was able to identify the optimal design parameters. All the conclusions derived from the previous 3D ventilated room are valid for this case.

4. Discussion

This study found that the constant step size was case dependent, as shown in Table 4. The reason may be that the relationship between the objective function and various design parameters cannot be expressed simply. The relationship is non-linear, coupled with multiple parameters according to the Navier-Stokes equation. Thus, trial and error must be used to determine a proper constant step size for each case. The trial-and-error process is time consuming and may depend on the designer's experience and luck.

5. Conclusions

This investigation proposed the use of the CFD-based adjoint method with an adaptive step size for adjusting design parameters in the inverse design of an indoor environment. In the three ventilation cases that were used as examples, the method was able to identify optimal design parameters (air supply velocity and temperature at the inlet). The inverse design process was automatic, although it was possible for the design parameters to fluctuate during the design process.

The CFD-based adjoint method with a constant step size for adjusting design parameters was used as a reference. This method is also able to find the optimal design parameters, but it

is time consuming to search for the constant step size through a trial-and-error process. The computing speed depends on the designer's experience and luck. However, the convergence process was stable, and the design parameters did not fluctuate greatly.

Acknowledgements

The research presented in this paper was financially supported by the National Natural Science Foundation of China through Grant No. 51478302 and by the national key project of the Ministry of Science and Technology, China, on "Green Buildings and Building Industrialization" through Grant No. 2016YFC0700500.

References

1. N.E. Klepeis, W.C. Nelson, W.R. Ott, J.P. Robinson, A.M. Tsang, P. Switzer, J.V. Behar, S.C. Hern, and W.H. Engelmann, The National Human Activity Pattern Survey (NHAPS): A Resource for Assessing Exposure to Environmental Pollutants, *Journal of Exposure Analysis and Environmental Epidemiology*, vol. 11, pp. 231-252, 2001.
2. J.D. Spengler and Q. Chen, Indoor Air Quality Factors in Designing a Healthy Building, *Environment and Resources*, vol. 25, pp. 567-600, 2000.
3. W. Liu, T.F. Zhang, Y. Xue, Z.J. Zhai, J.H. Wang, Y. Wei, and Q. Chen, State-of-the-art Methods for Inverse Design of An Enclosed Environment, *Building and Environment*, vol. 91, pp. 91-100, 2015.
4. Q. Chen, Ventilation Performance Prediction for Buildings: A Method Overview and Recent Applications, *Building and Environment*, vol. 44, pp. 848-858, 2009.
5. Y. Xue, Z.J. Zhai, and Q. Chen, Inverse Prediction and Optimization of Flow Control Conditions for Confined Spaces Using a CFD-Based Genetic Algorithm, *Building and Environment*, vol. 64, pp. 77-84, 2013.
6. C. Othmer, A Continuous Adjoint Formulation for the Computation of Topological and Surface Sensitivities of Ducted Flows, *International Journal for Numerical Methods in Fluids*, vol. 58, pp. 861-877, 2008.
7. J.L. Lumley, The Structure of Inhomogeneous Turbulent Flows, *Atmospheric turbulence and radio wave propagation*, pp. 166-178, 1967.
8. Q. Chen, Z. Zhai, X. You, and T. Zhang, *Inverse Design Methods for Built Environment*, Taylor & Francis Group, 2017.
9. L. Armijo, Minimization of Functions Having Lipschitz Continuous First Partial Derivatives, *Pacific Journal of Mathematics*, vol. 16, pp.1-3, 1966.
10. M. Towara and U. Naumann, A Discrete Adjoint Model for OpenFOAM, *Procedia Computer Science*, vol. 18, pp. 429-438, 2013.
11. M. Zeinalpour, K. Mazaheri, and A. Irannejad, Turbine Blade Aerodynamic Optimization on Unstructured Grids Using a Continuous Adjoint Method, *Proceedings of the ASME 2012 International Mechanical Engineering Congress and Exposition*, Houston, Texas USA, 2012.
12. E.M. Papoutsis-Kiachagias, S.A. Kyriacou, and K.C. Giannakoglou, The Continuous Adjoint Method for the Design of Hydraulic Turbomachines, *Computer Methods in Applied Mechanics and Engineering*, vol. 278, pp. 621-639, 2014.
13. O. Soto and R. Lohner, General Methodologies for Incompressible Flow Design Problems, *39th Aerospace Sciences Meeting and Exhibit*, 2001.
14. W. Liu and Q. Chen, Optimal Air Distribution Design in Enclosed Spaces Using an Adjoint Method, *Inverse Problems in Science and Engineering*, vol. 23, pp.760-779, 2015.

15. A.A. Goldstein, On Steepest Descent, *Journal of the Society for Industrial & Applied Mathematics*, vol. 1, pp.147-151, 1965.
16. M.N. Vrahatis, G.S. Androulakis, J.N. Lambrinosa, and G.D. Magoulas, A Class of Gradient Unconstrained Minimization Algorithms with Adaptive Stepsize, *Journal of Computational and Applied Mathematics*, vol. 114, pp. 367-386, 2000.
17. D.I. Papadimitriou and K.C. Giannakoglou, One-Shot Shape Optimization Using the Exact Hessian, *Fifth European Conference on Computational Fluid Dynamics*, Lisbon, Portugal, 2010.
18. S.B. Hazra, Multigrid One-shot Method for Aerodynamic Shape Optimization, *Pamm*, vol. 30, pp. 1527-1547, 2008.
19. W.K. Anderson and V. Venkatakrishnan, Aerodynamic Design Optimization on Unstructured Grids with a Continuous Adjoint Formulation, *Computers and Fluids*, vol. 28, pp. 443-480, 1999.
20. B.J.M. Ortega and W.C. Rheinboldt, *Iterative Solution of Nonlinear Equations in Several Variables*, Academic Press, NewYork, 1970.
21. G.K. Wen, Y.B. Dasril, I.B. Mohd, and M.B. Mamat, A Class of Steepest Descent Method with Fixed Range of Step Size, *World Applied Sciences Journal*, vol. 20, pp. 637-642, 2012.
22. Y. Fang, H. Shao, J. Zhao, and T. Wu, A Bi-dimensional Search-based Algorithm for Unconstrained Optimization Problems, *International Joint Conference on Computational Sciences & Optimization*, pp.500-503, 2012.
23. W.W. Hager and S. Park, The Gradient Projection Method with Exact Line Search, *Journal of Global Optimization*, vol. 30, pp. 103-118, 2004.
24. Z. J. Shi and J. Shen, New Inexact Line Search Method for Unconstrained Optimization, *Journal of Optimization Theory and Applications*, vol.127, pp. 425-446, 2005.
25. P. Wolfe, Convergence Conditions for Ascent Methods. *Siam Review*, vol. 11, pp. 226-235, 1969.
26. Q. Chen, Comparison of Different k-ε models for Indoor Air Flow Computations, *Numerical Heat Transfer, Part B: Fundamentals*, vol. 28, pp. 353-369, 1995.
27. OpenFOAM. The Open Source CFD Toolbox, http://www.openfoam.com, 2012.
28. W. Zhang and Q.Y. Chen, Large Eddy Simulation of Natural and Mixed Convection Airflow Indoors with Two Simple Filtered Dynamic Subgrid Scale Models, *Numerical Heat Transfer, Part A: Applications*, vol. 37, pp. 447-463, 2000.
29. D. Blay, S. Mergui, and C. Niculae, Confined Turbulent Mixed Convection in the Presence of a Horizontal Buoyant Wall Jet, *Fundamentals of Mixed Convection, ASME HTD*, vol. 213, pp. 65-72, 1992.
30. M. Wang and Q.Y. Chen, Assessment of Various Turbulence Models for Transitional Flows in Enclosed Environment, *HVAC&R Research*, vol. 15, pp. 1099-1119, 2009.
31. X.X. Yuan, Q.Y. Chen, L.R Glicksman, Y.Q. Hu, and X.D. Yang, Measurements and Computations of Room Airflow with Displacement Ventilation, *ASHRAE Transactions*, vol. 105, pp. 340-352, 1999.

Tables

Table 1. Air supply parameters obtained through inverse design of the 2D cavity

	$V_{x,\ inlet}$ (m/s)	$V_{y,\ inlet}$ (m/s)	T_{inlet} (K)	Objective function
Experimental data [29]	0.57	0	288.15	-
With adaptive step size	0.581	0.01	288.35	0.024
With constant step size	0.583	0	288.6	0.026

Table 2. Air supply parameters determined through inverse design of the 3D room

	$V_{x,\ inlet}$ (m/s)	$V_{y,\ inlet}$ (m/s)	$V_{z,\ inlet}$ (m/s)	T_{inlet} (K)	Objective function
Experimental data [30]	1.366	0	0	295.35	0
With adaptive step size	1.43	-0.007	5.2E-6	295.28	0.024
With constant step size	1.418	-0.0015	0.02	295.26	0.022

Table 3. Air supply parameters determined through inverse design of the 3D office

	$V_{x,\ inlet}$ (m/s)	$V_{y,\ inlet}$ (m/s)	$V_{z,\ inlet}$ (m/s)	T_{inlet} (K)	Objective function
Experimental data [31]	0.09	0	0	290.15	-
With adaptive step size	0.0894	1.37 E-4	9.2e-7	290.20	0.00015
With constant step size	0.0907	-4.86E-7	1.38E-7	289.95	0.000497

Table 4. Constant step sizes for the three inverse design cases

Case	Constant step size for air velocity	Constant step size for air temperature
2D ventilated cavity	10	3
3D ventilated room	100	50
3D ventilated office	50	2

Figures

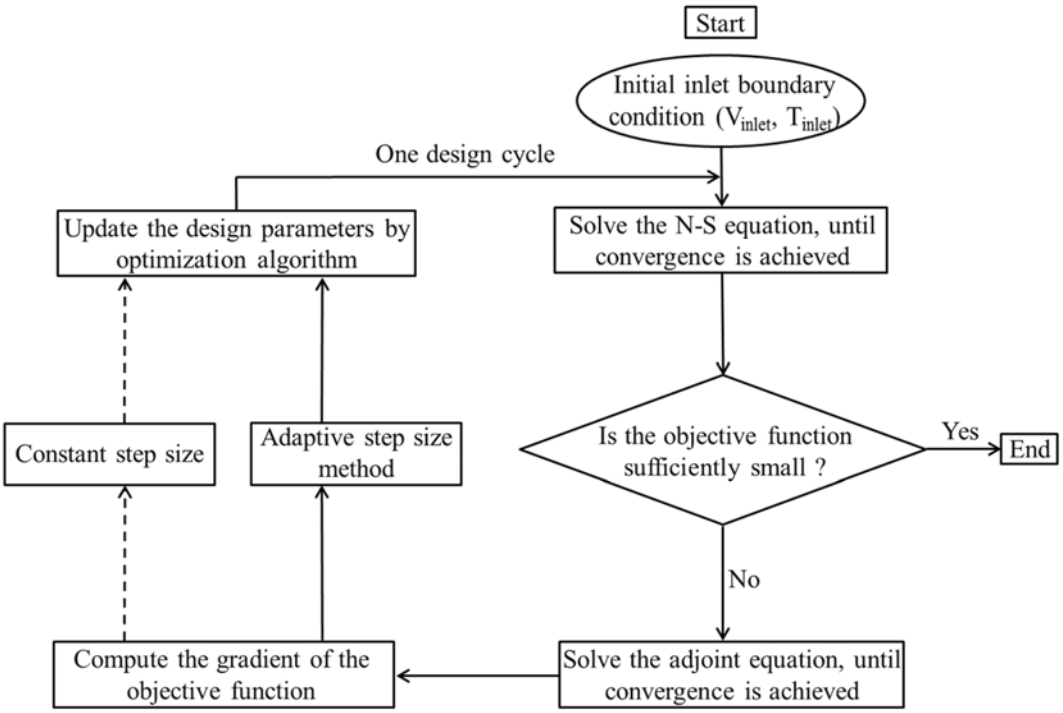

Figure 1. Flow chart of the CFD-based adjoint method

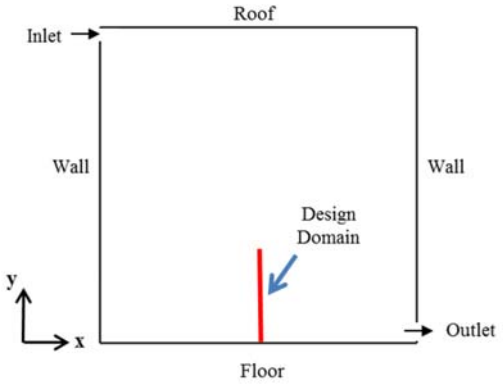

Figure 2. Schematic of the 2D ventilated cavity

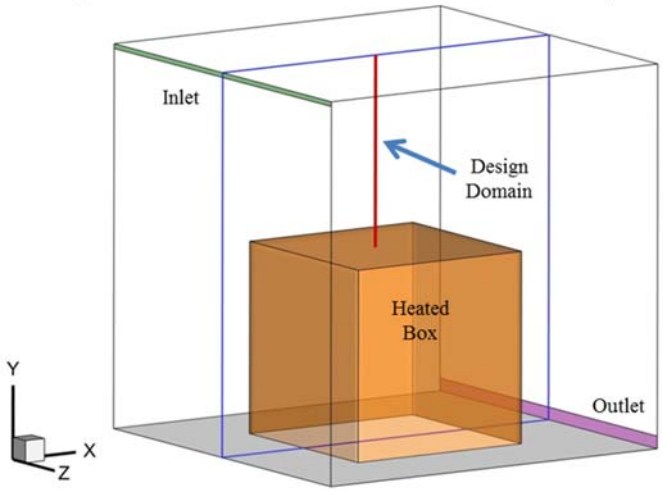

Figure 3. Schematic of the 3D ventilated room

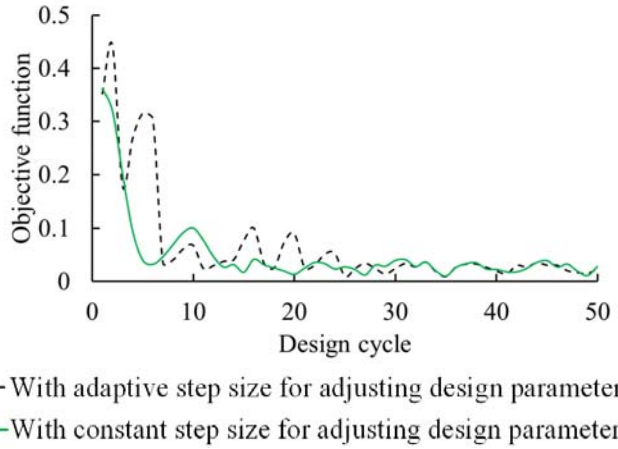

Figure 4. Change in the objective function with the design cycle

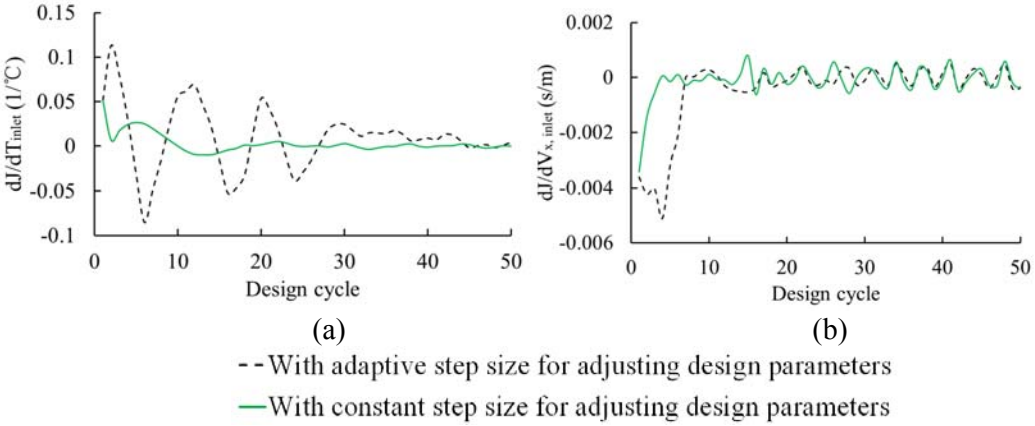

Figure 5. Convergence process of the gradient of the objective function with the design cycle

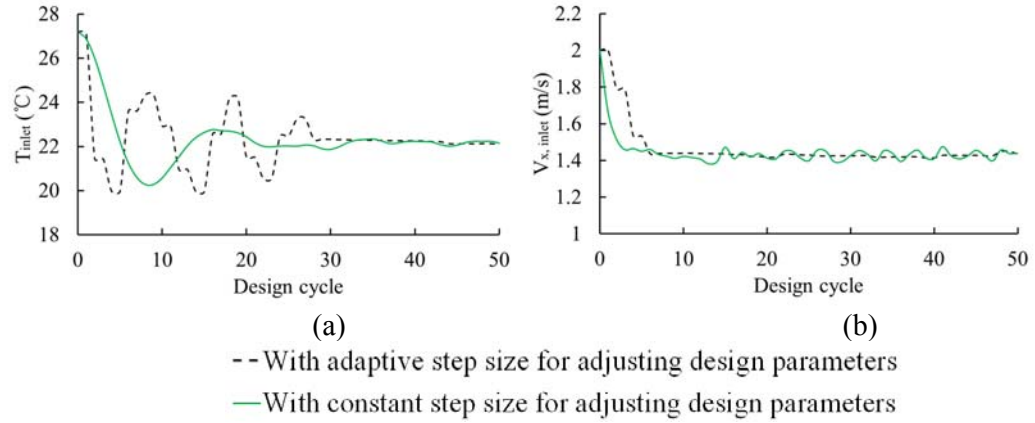

Figure 6. Convergence process of the design parameters with the design cycle

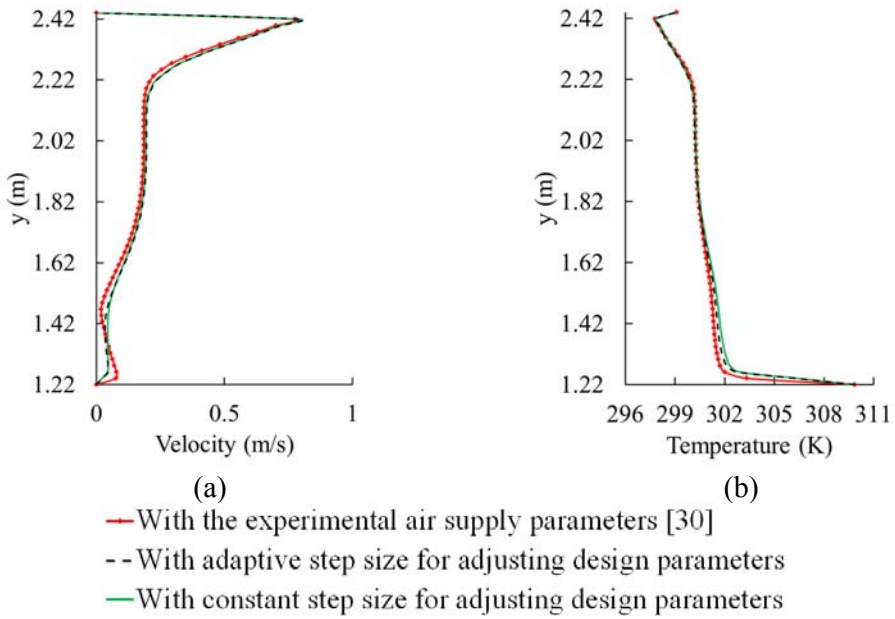

Figure 7. Comparison of (a) the air velocity profiles and (b) the temperature profiles in the design domain: simulated with the experimental air supply parameters, calculated with the adaptive step size, and calculated with the constant step size.

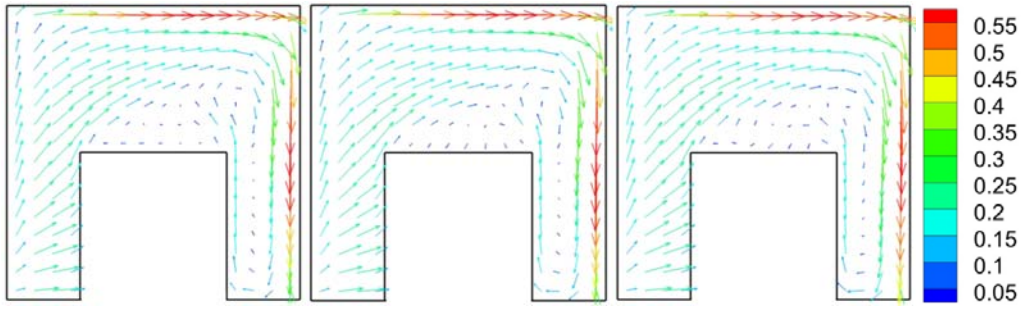

Figure 8. Comparison of the air velocity distributions with the air supply parameters (a) measured in the experiment, (b) calculated with the adaptive step size, and (c) calculated with the constant step size at the mid-z cross section.

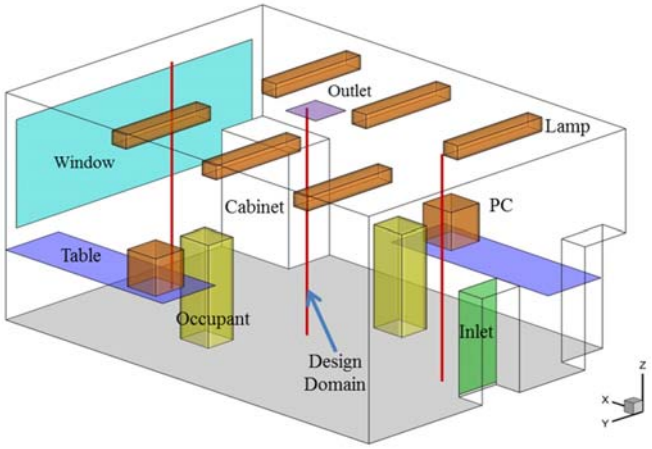

Figure 9. Schematic of the three-dimensional ventilated office

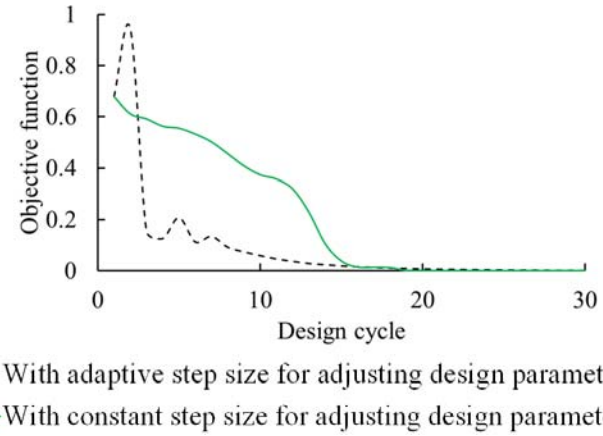

Figure 10. Change in the objective function with the design cycle

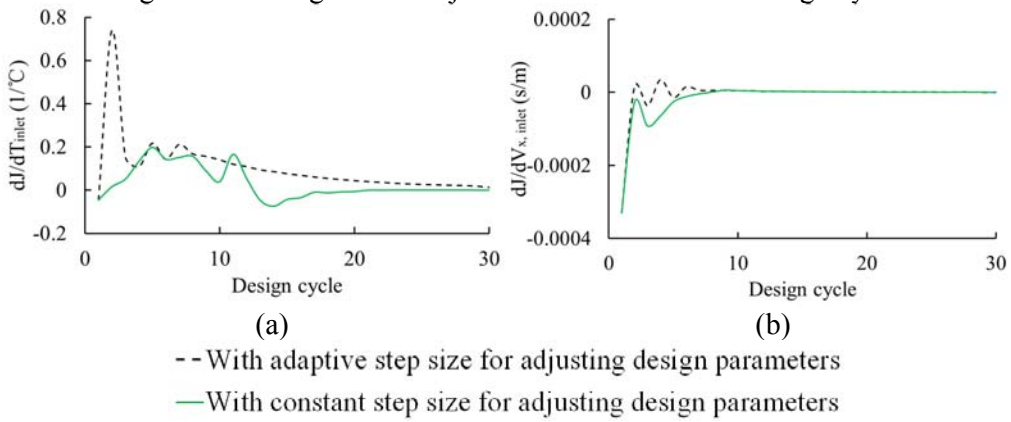

Figure 11. Change in the gradient of the objective function over the design parameters with the design cycle